Original article

Simultaneous Effects of Airflow and Temperature Increase on Water removal in Bio-drying

Geun-Yong Ham[1], Dong-Hoon Lee [2], Toshihiko Matsuto [1*], Yasumasa Tojo [1], Jae-Ram Park [2]

[1] Laboratory of Solid Waste Disposal Engineering, Faculty of Engineering, Hokkaido University, Kita 13, Nishi 8, Kita-ku, Sapporo, Hokkaido 060-8628, Japan

[2] Department of Environmental Engineering, University of Seoul, 163 Seoulsiripdaero, Dongdaemun-gu, Seoul 02504, Republic of Korea

Geun-Yong Ham: gyham127@gmail.com
Dong-Hoon Lee: dhlee@uos.ac.kr
Yasumasa Tojo: tojo@eng.hokudai.ac.jp
Jae-Ram Park: fuel3079@nate.com

* Corresponding author. Tel./fax: +81 11 706 6825
E-mail address: matsuto@eng.hokudai.ac.jp

ABSTRACT

Bio-drying MBT is a type of mechanical biological treatment (MBT) system, whereby the aerobic biological process is first used to remove moisture, which is followed by the mechanical separation to recover material and energy as a solid recovered fuel (SRF). Among various parameters of this process, the simultaneous effects of airflow rate and organic contents were examined in this study. A 25 L acrylic column reactor was filled with simulated waste. Temperature and humidity of the air inlet and outlet were continuously monitored, and CO_2 concentrations in outlet air were periodically analyzed to observe aerobic biodegradation as well as metabolic water generation. Based on the data, the different water removal contributions by airflow and biodegradation were compared and finally evaluation of the inter-dependence of parameters and feedback effect in the bio-drying process was carried out. While the biodegradation of organics induced a significant amount of water removal due to increased temperature, high organic content has a negative effect on water removal by generating metabolic water. Water removal by air replacement is greater than that associated with temperature increases caused by biodegradation. However, excessive airflow rate can terminate biodegradation by drastically lowered moisture content even though organics remained.

Keywords: Bio-drying, Organic content, Airflow rate, Water removal rate

Introduction

Historically, most EU countries disposed of substantially mixed municipal solid waste (MSW) in landfills without any type of pretreatment. High proportions of biodegradable wastes have been discarded in landfills, which resulted in a need for long-term care to manage the leachate and landfill gas emission caused from the biodegradation of organic matter in the waste [1]. To deal with this issue, in the late 1990s, the European Commission established the Landfill Directive (99/31/EC) [2], which required the diversion of biodegradable waste from landfills. In response to this directive, mechanical biological treatment (MBT) systems have emerged to reduce the amount of biodegradable waste sent to the landfill. A typical MBT system begins with mechanical separation of mixed MSW, which is then followed by biological treatment to remove the organics and thermal treatment for the remaining combustible fraction. The biologically and/or thermally stabilized residue from these processes is sent to a landfill for disposal. Biogas is recovered when the organic fraction is treated by anaerobic digestion, and energy is recovered as a solid fuel or through thermal treatment, and dry recyclables are also recovered [3].

Bio-drying MBT is a type of MBT system, in which an aerobic biological process is first used to remove moisture, followed by mechanical separation to recover material and energy as a solid recovered fuel (SRF). SRFs can be burned in cement kilns or other co-combustion power plants as a fuel, which conserves the conventional energy sources typically used for those kinds of operations [4, 5].

In a previous study on bio-drying, the effects of several parameters were examined, including aeration (airflow rate (AFR), frequency), waste properties (waste type, moisture content, organic content (OC)), and bulking agents (type, mixing ratio) used to adjust the OCs or moisture contents. Among them, the AFR and OC have been considered as the primary parameters, and these two parameters were investigated in this study. The simultaneous effects of the AFR and OC were also studied by Huiliñir and Villegas and Colomer-Mendoza et al. [6, 7]. Huiliñir and Villegas used sludge from a wastewater treatment plant used for the slaughterhouse and investigated the AFR (1, 2, and 3 L/min·kg-TS) and OC by changing the ratio of the bulking agents (10%, 23%, and 33%), which resulted in different initial moisture content values of 59%, 68%, and 78%, respectively. Colomer-Mendoza et al. studied AFR (0.88 to 6.42 L/min·kg-TS) and the bulking agent ratio (0% and 15% of mixture) in the bio-drying of garden waste.

Other studies have investigated AFR, OC, and other parameters. Adani et al. studied AFR (0.1–0.4 L/min·kg-TS) in bio-drying of MSW [8], and Navaee-Ardeh et al. investigated AFR (25–75 m^3/h) in a bio-drying process that utilized paper and pulp mill sludge as the feedstock [9]. While other studies have been conducted as batch processes, bio-dried sludge was recirculated in a study by Navaee-Ardeh et al. [9]. The effect of OCs was investigated by Yang et al. using different concentration of glucose and ground food waste that were mixed with bio-dried sludge for inoculation [10]. In addition to the AFR and bulking agent ratio, the type of bulking agent, such as sawdust, wood pellets, straw, and corncob [11–13] and initial moisture content for sewage sludge bio-drying [11], and inoculation ratio [13] have also been studied.

In the bio-drying process, moisture is removed by the combined actions of aeration and biodegradation. Generated metabolic heat increases the temperature inside the reactor, and this facilitates the moisture evaporation from the waste. Air then carries the evaporated vapor and discharges it to the atmosphere. Measuring the weight of the waste before and after the experiment is the most common method of determining changes in moisture content. However, this only shows the change in the water amount. To estimate certain ongoing phenomena during the process, temperature, relative humidity in the airflow, and CO_2 concentrations must be continuously measured, and metabolic water generation should be taken into account. Among the previous studies, such continuous monitoring was performed by Cai et al., Huiliñir and Villegas and Navaee-Ardeh et al. [6, 9, 14]. However, Cai et al. and Huiliñir and Villegas estimated the metabolic water generation through the measurement of VS changes by periodic waste sampling, whereas Navaee-Ardeh et al. estimated metabolic water generation by changes in the CO_2 concentration, but only the AFR was changed as an experimental condition.

Compared with the previously conducted studies that we reviewed, the novelty of our approach is characterized by the monitoring of the simultaneous effects of OC and AFR to balance moisture, including metabolic water generation determined by continuous measurement of the airflow. To establish the moisture balance, inlet and outlet flow of moisture were estimated by continuous measurement of temperature and relative humidity of the air. CO_2 concentrations in the outlet air were periodically analyzed to observe aerobic biodegradation as well as metabolic water generation. Furthermore, contributions from the AFR and temperature increase on water removal were quantitatively compared.

Materials and methods

Experimental equipment

Fig. 1 Schematic view of the reactor used in the bio-drying experiment

As shown in Fig. 1, the reactor used in this study was a 25 L acrylic cylindrical reactor with a diameter of 20 cm and a height of 70 cm. The reactor was filled with simulated wastes on a perforated base plate to ensure uniform air distribution from 30 to 60 cm in the reactor. The upper portion was covered with an acrylic lid with a hole for air exhaust. The reactor was insulated with a 5 cm thick layer of Styrofoam. A blower was connected to the bottom of the reactor with Teflon tubing. Ambient air was introduced via the blower and moved upward through the reactor toward the exhaust port in the lid. Heat loss through reactor wall by conduction and radiation is negligible because the loss is less than 1 % of energy consumption for evaporation and temperature increase of air and solid materials in lab-scale bio-drying reactor insulated with 100-mm of a hollow cotton wall [15].

The experiments were conducted from March to May 2015 and July to August 2016. All the experiments were conducted in a temperature-controlled room at 30 °C ±1 °C. The reactor was placed on an electronic scale (FG-60KBM-H, AND, Korea), and the total weight was measured and manually recorded at 12 h intervals. Each experimental run was terminated when the temperature of outlet air reached that of the ambient air.

Measurement and analysis

The temperature and humidity of the inlet and outlet air were monitored by a humidity-temperature meter (TES-1365, TES, Taiwan). Three temperature sensors were installed (two inside the reactor and the one at the outlet port in the lid) and connected to a thermometer (TES-1384, TES, Taiwan). The data logging interval was set to 4 min for monitoring both ports. Inlet and outlet gas were sampled every 12 h to quantify CO_2 concentrations by gas chromatography (GC-2014, Shimadzu, Japan). An in-line gas flow meter (RMA, Dwyer, United States) was used to monitor the AFR.

At the end of all experimental runs, simulated waste was taken from the reactor, and the final weight was measured. After weighing, the moisture content of the product was determined by oven drying (forced convection drying oven, Chang Shin scientific co., Korea) at 80 °C.

Experimental condition

In the experiment, commercial dog food (Prime Balance, Nutrena, Korea) was used to represent easily biodegradable matter in the simulated waste. Nakasaki et al. and Chang et al. reported that dry dog food can represent the easily biodegradable organic matter, and they demonstrated good reproducibility, which resulted in uniform properties at the beginning and end of the experiment [16, 17]. According to the nutrition level in the dog food used in this experiment, it consisted primarily of carbohydrates (70% d.w.), crude protein (14% d.w.), crude fat, crude fiber, and miscellaneous elements. Based on elemental compositions (C 44.7%, H 6.3%, N 2.4%, O 39.0%, ash 7.6% dry basis) determined by the authors, the chemical composition of the VS was estimated to be $C_{21}H_{36}O_{14}N$.

OC was controlled by changing the ratio of dog food to wood pellets and included 10%, 25%, 50%, 75%, and 100%, by mass. Although the dog food is not 100% biodegradable, its dry basis ratio is referred to as OC for the purpose of this study. The wood pellets were assumed to be non-degradable during the bio-drying process due to their relatively low biodegradability in the relatively short process time of the experiment [12]. As a simulated waste, 3.1 kg of the dog food and wood pellet mixture with the previously mentioned ratios was placed in the column reactor, and the initial moisture content was set at 40% by adding distilled water. Forty percent of the initial moisture content was determined after measuring the field capacity of the dog food. With over 50% of moisture content, the dog food easily becomes broken down. Return activated sludge, which was collected from a commercial wastewater treatment facility, was injected to inoculate the simulated waste and was equal to 10% of the dog food mass on a dry basis.

Regarding aeration, it has been suggested that the recommended aeration rates depend on the substrate in the composting process [18]. The bio-drying process is a modified composting process but focused more on water removal. Therefore, a slightly higher range of AFR can be applied. In this study, the operation range applied in the past study, 0.4–1.1 L/min·kgVS, was used by referring to Adani et al. and Colomer-Mendoza et al. [7, 8]. When the initial OC was 100%, 0.4 L/min·kgVS was multiplied by 3.1 kg, resulting in a value of 1.2, which corresponded to approximately 1 L/min. Therefore, the AFRs selected for experimental analysis were set at 1, 2, and 3 L/min.

Table 1. Different variables and initial conditions in the experiments

Table 1 summarizes the experimental conditions employed in this study. All the experimental runs were identified by the initial OC and AFR, such as "10-1" (i.e., 10% OC and a flowrate of 1 L/min). The average relative humidity (RH) of the inlet air in each experiment depended on the season. Table 1 presents the total days of operation, initial organic matter (dog food), and final organic matter and moisture content. The equations presented in next section were used to estimate final values.

Model

Model equations

The moisture balance in the reactor can be described by Eqs. (1) and (2).

$$\Delta w_{nom}\ (kg/h) = (V_{out} \times X_{out} \times 10^{-3}) - (V_{in} \times X_{in} \times 10^{-3}) \qquad (1)$$

$$\Delta w_{act}\ (kg/h) = \Delta w_{nom} - \Delta w_{gen} \qquad (2)$$

where V is AFR in m^3/h, and X represents the water vapor content per unit volume of air, in g/m^3. Eq. (1) is the water removal rate determined by the difference between moisture measured at the inlet and outlet of the airflow on a per hour basis, but it was nominal without considering the metabolic water generation (Δw_{gen}). Therefore, the actual water removal rate, Δw_{act}, was calculated using Eq. (2).

Table 2. Equations used for mass and heat balance

Table 2 summarizes other equations used in the model, and the nomenclature is provided at the end of this paper. The outlet AFR (V_{out}) was calculated by considering the change in air density of the inlet airflow (V_{in}) (Eq. (3)). X, which denotes the water vapor content per volume of air, was calculated using Eq. (4) as a function of water vapor pressure (pv). The maximum value of water vapor pressure that can be reached at any temperature is defined as the saturated water vapor pressure (pvs). The ratio between pv and pvs is the RH.

For biodegradation, it was assumed that the organics were fully degraded which can thus be expressed by Eq. (7). CO_2 generation rate ($\triangle C_{gen}$) was estimated by the difference between the CO_2 concentrations in the air at the inlet and outlet (Eq. (8)). Degraded organics and generated metabolic water per unit time can be calculated using Eqs. (9) and (10), which are based on Eq. (8).

The mass of organics (M_O) and moisture (W) at a particular time or its change during a particular period of time can be estimated by the integration of each rate ($\triangle M_O$, $\triangle w$). Moisture content (MC) can be calculated by the ratio between water mass to total waste mass at a specific time, and OC was estimated by the ratio of M_O to total dry mass.

The rate of heat generation, ΔQ_{gen}, was calculated using Eq. (11) by multiplying the reaction heat of the degraded organics. Spoehr and Milner suggested the empirical method for calculating the heat of combustion for any type of organic matter is expressed by Eq. (12),

$$Q\ (kJ/kg) = \left(127 \times \frac{\{100\times(2.66\times C\% + 7.94\ \times H\% - O\%)\}}{398.9} + 400\right) \times \frac{4.184\ kJ}{1\ kcal} \qquad (12)$$

where Q is the heat of combustion for degraded organics, and C%, H%, and O% are the weight percentages of carbon, hydrogen, and oxygen, respectively, on an ash-free basis [19]. For the dog food used in this study, its heat of combustion was estimated to be 20406 kJ/kg. Heat transfer in the inlet and outlet airflow (ΔQ_{in} and ΔQ_{out}) is calculated using the sum of dry air and water vapor enthalpy by applying Eq. (13).

Example of model output

Fig. 2 Experimental data and model output of run "50-3" (a) Temperature and CO_2 concentration profiles (Measured), (b) Rate of water mass changes in balance (Estimated), (c) Heat profiles (Estimated)

As an example of model output, Fig. 2 shows the time profile for the run 50-3 (i.e., 50% of initial OC and a 3 L/min inlet AFR). The average inlet RH was 14.0% (see Table 1). Values in Fig. 2a were measured, and the others were calculated using the model in Table 2. During the initial period when biodegradation had not yet begun, which is referred to as "w/o BIO" in the figure, T_{in} and T_{out} were held constant, and the slight decrease of T_s was due to heat loss associated with evaporation.

After one day, CO_2 concentrations began to increase, which is indicative of a biodegradation process at work. The integrated area under the CO_2 curve presents the extent of organic degradation. During the biodegradation period, referred to as "w/ BIO," nominal water removal rate (Δw_{nom}) increased as T_{out} increased. This is one of the fundamental features of bio-drying, though actual water removal rate (Δw_{act}) was decreased by metabolic water generation rate (Δw_{gen}).

Microbial biodegradation of organic matter gradually decreased after it peaked at its maximum. Either remaining OC or MC could have affected microbial activity, which is discussed in detail later. Fig. 2c shows the heat balance. The difference between ΔQ_{gen} and ΔQ_{out} was indicative of the heat used for evaporation or loss from the reactor.

Reliability of model

Fig. 3 Comparison of actual removed water mass (W_{act}) between experiment and model during entire experimental period

The mass of removed water (W_{act}) calculated by the model (integration of $\triangle w_{act}$) was compared with that of the experiments during entire experimental period, as shown in Fig. 3, where each label indicates the initial OC. The magnitude of error is generally within 20%. Therefore, the model estimated the bio-drying phenomena reasonably well.

Discussion

Drying mechanism in the bio-drying process

Fig. 4 Temperature dependence of pvs and X_{sat} and increase of water vapor pressure (pv) in bio-drying process

Drying is a process of moisture transfer from the surface of waste to air. Evaporation is driven by the differences of water vapor pressure between the surface of the waste and air. The required heat for evaporation is obtained from the surroundings. Since the RH of the outlet air was always 100% in all experimental runs, pv at inlet temperature increase to pvs at outlet temperature. The driving force of evaporation can be expressed as the gap between two points, i.e., outlet on the pvs curve and inlet in Fig. 4. As the temperature increased, the pvs in the air increased so as X_{sat}.

The change of pv (water vapor pressure) in the air from the inlet to outlet is schematically shown by the broken arrow in Fig. 4. In w/o BIO period, before biological decomposition occurred, there were no increases in temperature due to the absence of heat associated with biodegradation. Consequently, the water vapor pressure pv in the air increased only up to the pvs (saturated water vapor pressure) at the same temperature when it was introduced into the reactor. However, once biodegradation proceeded under w/ BIO period, the heat generation increased the waste temperature. Simultaneously, the initial driving force of evaporation increased dramatically due to a high pvs, which was indicative of an increase in the water content in the outlet air, X_{out}.

Water removal rate is increased with biodegradation as shown in Fig. 4, and the airflow carried saturated vapor out of the reactor. In w/o BIO period, only the influence of AFR can be discussed, and the relationship $1 - \left({}^{RH}/_{100}\right)$ = (Δw_{act}=Δw_{nom} in this case) for different AFR by taking $1 - \left({}^{RH}/_{100}\right)$ as x-axis (Fig. 5). The higher the AFR, the more water was removed, and simultaneously, the lower the RH of the inlet air, which resulted from the large amount of water removal associated with the increasing gap between the pvs and the pv.

Fig. 5 Relations between water removal rate and RH of inlet air under different AFR during w/o BIO period

In Fig. 5, a regression line for AFR = 1 L/min was first determined by assuming the removal rate was zero at an RH of inlet air = 100%, whereby the lines for AFR = 2 L/min and 3 L/min are simply multiplied by 2 and 3, respectively. That is, AFR has simply the replacement effect of saturated air in the reactor.

Biodegradation of organic matter and its limitation

Fig. 6 CO_2 generation rate and moisture content profiles during entire experimental period (a) AFR 1 L/min, (b) AFR 3 L/min

Different initial conditions of the OC and AFR induced different biodegradation characteristics. To observe the extent of biodegradation, the CO_2 generation rate ($\triangle C_{gen}$) and MC profiles are shown in Fig. 6. The $\triangle C_{gen}$, expressed in kmol/h, is calculated using the AFR and CO_2 concentrations in the outlet air (Eq. (8)). The integration of each curve is proportional to the amount of degraded OC. The numbers in parenthesis indicate the initial and final OC, which are defined by the ratio of organics to total dry solids.

CO_2 generation rate curves of all runs were bell-shaped and had longer tails at lower AFRs and higher OC values. In runs with the AFR set at 3 L/min (Fig. 6b), biodegradation did not continue very long compared to the runs with lower AFRs because microbial activity was limited by low levels of MC, even though sufficient OC was still available (i.e., 19%, 42%, and 83% corresponding to initial OC values of 25%, 50%, and 100%, respectively). The low MC was caused by high AFR values that rapidly carried out all vaporized water.

By contrast, in runs using an AFR of 1 L/min, biodegradation continued for a longer period of time until the OC decreased to 12% and 27%, corresponding to initial OC values of 25% and 50%, respectively. During the experiment, MC was maintained around 40% due to the low AFR. In this case, biodegradation was terminated due to the low concentrations of organics, not by moisture. In run 100-1, biological degradation ceased in spite of 67% of the organics remaining because the feed material was composed only of dog food. Without bulking material (i.e., wood pellets), the dog food stuck together, and the biodegradation was limited due to a reduction in the contact area associated with short-circuiting of the airflow around larger masses of dog food.

Effects of air flow and biodegradation

Fig. 7 Conceptual diagram of water removal rate in the bio-drying process

Fig. 7 depicts a conceptual diagram of the water removal rate in the bio-drying process. Metabolic water generation rate ($\triangle w_{gen}$) is depicted as a negative value to indicate added water by bio-drying process, and the water removal rate during the w/o BIO period is denoted as $\triangle w_{air}$. From this figure, the following three water removal rates during the w/ BIO period can be defined.

Effect of airflow: $\triangle w_{air}$

Effect of temperature increase (nominal): $\triangle w_{nom}$-$\triangle w_{air}$

Effect of temperature increase (actual): $\triangle w_{nom}$ - $\triangle w_{air}$ - $\triangle w_{gen}$

Given that the time profile was different among experiments (refer to Fig. 6), a comparison of the water removal rate and maximum temperature of the simulated waste at the peak point of CO_2 concentration for all the runs is shown in Fig. 8.

Fig. 8 Water removal rate defined in Fig. 7 at the peak point of CO_2 concentration (a) AFR 1 L/min, (b) AFR 3 L/min

Except for the runs with 10% of the initial amount of OC, where less heat generation occurred due to the small amount of organic matter, the maximum temperature of the outlet air ranged between 45 °C and 50 °C. The metabolic water generation rate, $\triangle w_{gen}$, remained virtually constant regardless of AFR and initial OC. A constant $\triangle w_{gen}$ indicates that biodegradation rate at peak time did not depend on the experimental conditions in this study.

Compared with the Fig. 8a and Fig. 8b, the nominal effect of temperature increase ($\triangle w_{nom}$-$\triangle w_{air}$) on water removal remarkably increased as the AFR increased, but so did $\triangle w_{air}$. Airflow replace the saturated vapor as mentioned in previous section, so replaced volume of air is proportionately increased with AFR in unit time. To exclude the increased effect of replaced air, each water removal rate was divided by the AFR, ($\triangle w_{nom}$-$\triangle w_{air}$) / V and $\triangle w_{air}$ / V, as shown by the broken line in Fig. 8b, and these were similar to the result when the AFR was 1 L/min. Therefore, the effect of airflow was higher than the temperature increase.

As a result, the actual water removal rate, which was determined by the difference between ($\triangle w_{nom}$−$\triangle w_{air}$) and $\triangle w_{gen}$ curves also increased with AFR because $\triangle w_{gen}$ remained virtually constant regardless of the AFR.

Total water removal during w/ BIO period

The previous section discussed the water removal rate at the peak point of CO_2 concentration. However, the efficiency of drying should be evaluated by the total amount of removed water throughout the experiment period. In Fig. 9, the integrated amount of water removal during the w/ BIO period is shown.

Fig. 9 Removed water mass during w/ BIO period (a) Comparison of nominal removed water mass (W_{nom}) and actual removed water mass (W_{act}), (b) Effect of temperature increase (W_{nom}−W_{air}, W_{nom}−W_{air}−W_{gen}) on water removal compared with the effect of airflow (W_{air})

As shown in Fig. 9a, the amount of nominal removed water mass, W_{nom}, increased as the initial OC increased. This was caused by the difference in the duration of aerobic biodegradation. In other words, as shown in Fig. 6a, when the initial OC is high, the aerobic reaction continued for a longer period of time. Therefore, the amount of moisture removal increased with a higher water vapor pressure (pvs) and with a longer duration of saturated vapor replaced by airflow.

There was little difference by AFR in W_{nom} (Fig. 9a), because the shorter duration of the aerobic reaction associated with high AFR was made up or vice versa (see Fig. 6). The duration of active biodegradation is shown in Fig. 9a. On the other hand, W_{act} significantly decreased in lower AFR runs because of the considerable amount of metabolic water generation by long biodegradation. Meanwhile, aerobic biodegradation was terminated due to low MC (see Fig. 6b) which resulted from the significant replacement of moisture by a high AFR.

Finally, the effect of temperature increase compared with the effect of AFR on water removal is presented in Fig. 9b. ($W_{nom}-W_{air}$) refers to the water mass removed by increases in temperature and ($W_{nom}-W_{air}-W_{gen}$) shows the ultimate amount of water removed, including the negative effect of added metabolic water. All points were plotted against W_{air}, which is the water removal solely associated with aeration. OC values of 10%, 50%, and 100% are plotted for comparison among all runs, and each OC is represented with different marks.

In each AFR condition, the higher the initial OC, both W_{air} and ($W_{nom}-W_{air}$) increased due to the longer period of elapsed time, which maximizes the effect of increases in temperature. However, when metabolic water is taken into account, the actual water removal ($W_{nom}-W_{air}-W_{gen}$) by biodegradation decreased at lower AFR values, which was especially true in runs 10-1 and 50-1 that showed negative values or values close to zero due to the reduced replacement effect. In case 100-1, agglomerated feed materials interrupted the air passage, and this resulted in less biodegradation as well as less metabolic water generation. When comparing the x- and y-axis values of ($W_{nom}-W_{air}-W_{gen}$), which are equal to the actual water removal, the effects of temperature increase associated with biodegradation on water removal were always lower than those associated with air replacement.

Conclusion

Fig. 10 Overall water removal mechanism in the bio-drying process

Fig. 10 summarizes the overall water removal mechanism in the bio-drying process under different initial conditions, including variations in OC (organic content), AFR (airflow rate), and RH (relative humidity) of the inlet air. Evaporation is driven by the difference between the pvs (saturated water vapor pressure) of the waste surface and the pv (water vapor pressure) in the passing air, and this driving force increased either due to temperature increases associated with biodegradation or the dryness of introducing air. However, high OC was a negative contribution with respect to water removal due to the generation of metabolic water. On the other hand, saturated vapor in the reactor was carried out by airflow, so high AFR enhanced the water removal rate. Water removal associated with air replacement was generally greater than that associated with temperature increases caused by biodegradation. But excessive AFR would terminate biodegradation due to the reduction in MC even though organics remained.

In the bio-drying process, all the parameters are interdependent, and there are several feedback loops as previously mentioned. The findings of this study can be used for the design and operation of a full-scale system.

Appendix

Nomenclature			
Symbol		**Unit**	**Definition**
State variables	t	days	Time
	T	°C	Temperature
	V	m^3/h	Airflow rate
	CO_2	%	CO_2 concentration
	X	g/m^3	Water vapor per unit air volume
	RH	%	Relative humidity
	ρ_a	kg/m^3	Density of dry air
	pv	Pa	Water vapor pressure
	pvs	Pa	Saturated water vapor pressure
Decomposition	M_O	kg	Organic mass
	ΔM_O	kg/h	Organic degradation rate
	ΔC_{gen}	kmol/h	CO_2 generation rate
	OC	%	Organic content
Moisture	W	kg	Water mass
	Δw	kg/h	Water removal rate
	Δw_{gen}	kg/h	Metabolic water generation rate
	MC	%	Moisture content
Heat	ΔQ	kJ/h	Heat flow rate
	ΔQ_{gen}	kJ/h	Metabolic heat generation rate
	Q	kJ/kg	Heat of combustion for degraded organics
	h_{dry}	kJ/kg	Enthalpy of dry air
	h_{vapor}	kJ/kg	Enthalpy of water vapor

Subscript	Definition
in	Inlet
out	Outlet
s	Waste
nom	Nominal

act	Actual
air	Removed by airflow

Acknowledgement

This work was supported by the 2017 Research Fund of the University of Seoul

References

1. Brennan RB, Healy MG, Morrison L, et al (2016) Management of landfill leachate: The legacy of European Union Directives. Waste Manag 55:355–363. https://doi.org/10.1016/j.wasman.2015.10.010
2. European commission (1999) Council Directive 1999/31/EC on the landfill. Off J Eur Communities L182/14-23. https://doi.org/10.1039/ap9842100196
3. Juniper Consultancy Services Ltd (2005) Mechanical-Biological Treatment: A Guide for Decision Makers, Processes, Policies and Markets
4. Kanning K, Ketelsen K (2013) MBT – Best technology for treatment of moist MSW AD and / or biodrying prior to energy recovery. pp 328–342
5. Velis CA, Longhurst PJ, Drew GH, et al (2009) Biodrying for mechanical-biological treatment of wastes: A review of process science and engineering. Bioresour Technol 100:2747–2761. https://doi.org/10.1016/j.biortech.2008.12.026
6. Huiliñir C, Villegas M (2015) Simultaneous effect of initial moisture content and airflow rate on biodrying of sewage sludge. Water Res 82:118–28. https://doi.org/10.1016/j.watres.2015.04.046
7. Colomer-Mendoza FJ, Herrera-Prats L, Robles-Martínez F, et al (2013) Effect of airflow on biodrying of gardening wastes in reactors. J Environ Sci (China) 25:865–872. https://doi.org/10.1016/S1001-0742(12)60123-5
8. Adani F, Baido D, Calcaterra E, Genevini P (2002) The influence of biomass

temperature on biostabilization-biodrying of municipal solid waste. Bioresour Technol 83:173–179. https://doi.org/10.1016/S0960-8524(01)00231-0

9. Navaee-Ardeh S, Bertrand F, Stuart PR (2010) Key variables analysis of a novel continuous biodrying process for drying mixed sludge. Bioresour Technol 101:3379–3387. https://doi.org/10.1016/j.biortech.2009.12.037

10. Yang B, Zhang L, Lee Y, Jahng D (2013) Novel bioevaporation process for the zero-discharge treatment of highly concentratedorganic wastewater. Water Res 47:5678–5689. https://doi.org/10.1016/j.watres.2013.06.044

11. Yang B, Zhang L, Jahng D (2014) Importance of Initial Moisture Content and Bulking Agent for Biodrying Sewage Sludge. Dry Technol 32:135–144. https://doi.org/10.1080/07373937.2013.795586

12. Zhao L, Gu WM, He PJ, Shao LM (2011) Biodegradation potential of bulking agents used in sludge bio-drying and their contribution to bio-generated heat. Water Res 45:2322–2330. https://doi.org/10.1016/j.watres.2011.01.014

13. Song X, Ma J, Gao J, et al (2017) Optimization of bio-drying of kitchen waste: inoculation, initial moisture content and bulking agents. J Mater Cycles Waste Manag 19:496–504. https://doi.org/10.1007/s10163-015-0450-3

14. Cai L, Gao D, Chen T Bin, et al (2012) Moisture variation associated with water input and evaporation during sewage sludge bio-drying. Bioresour Technol 117:13–19. https://doi.org/10.1016/j.biortech.2012.03.092

15. Zhao L, Gu WM, He PJ, Shao LM (2010) Effect of air-flow rate and turning frequency on bio-drying of dewatered sludge. Water Res 44:6144–6152. https://doi.org/10.1016/j.watres.2010.07.002

16. Nakasaki K, Nag K, Karita S (2005) Microbial succession associated with organic matter decomposition during thermophilic composting of organic waste. Waste Manag Res 23:48–56. https://doi.org/10.1177/0734242X05049771

17. Chang JI, Tsai JJ, Wu KH (2005) Mathematical model for carbon dioxide evolution from the thermophilic composting of synthetic food wastes made of dog food. Waste

Manag 25:1037–1045. https://doi.org/10.1016/j.wasman.2005.01.018

18. Ahn HK, Richard TL, Choi HL (2007) Mass and thermal balance during composting of a poultry manure-Wood shavings mixture at different aeration rates. Process Biochem 42:215–223. https://doi.org/10.1016/j.procbio.2006.08.005

19. Spoehr HA, Milner H (1949) The chemical composition of Chorella; effect of environmental conditions. Plant Physiol 120–149. https://doi.org/10.1104/pp.24.1.120

Figure captions:

Fig. 1 Schematic view of the reactor used in the bio-drying experiment

Fig. 2 Experimental data and model output of run "50-3" (a) Temperature and CO_2 concentration profiles (Measured), (b) Rate of water mass changes in balance (Estimated), (c) Heat profiles (Estimated)

Fig. 3 Comparison of actual removed water mass (W_{act}) between experiment and model during entire experimental period

Fig. 4 Temperature dependence of pvs and X_{sat} and increase of water vapor pressure (pv) in bio-drying process

Fig. 5 Relations between water removal rate and RH of inlet air under different AFR during w/o BIO period

Fig. 6 CO_2 generation rate and moisture content profiles during entire experimental period (a) AFR 1 L/min, (b) AFR 3 L/min

Fig. 7 Conceptual diagram of water removal rate in the bio-drying process

Fig. 8 Water removal rate defined in Fig. 7 at the peak point of CO_2 concentration (a) AFR 1 L/min, (b) AFR 3 L/min

Fig. 9 Removed water mass during w/ BIO period (a) Comparison of nominal removed water mass (W_{nom}) and actual removed water mass (W_{act}), (b) Effect of temperature increase ($W_{nom}-W_{air}$, $W_{nom}-W_{air}-W_{gen}$) on water removal compared with the effect of airflow (W_{air})

Fig. 10 Overall water removal mechanism in the bio-drying process

Table 1. Different variables and initial conditions in the experiments

Experimental condition							
	Initial				Initial	Final	
Runs	OC	V	RH ± SD	Time	M_O	M_O	W
	%	L/min	%	days	kg	kg	kg
10-1	10	1	61.1 ± 4.7	19	0.314	0.000	1.842
25-1	25	1	23.8 ± 5.0	16	0.786	0.375	1.404
50-1	50	1	23.8 ± 5.5	16	1.571	0.879	1.420
75-1	75	1	15.0 ± 7.2	32	2.357	1.475	0.919
100-1	100	1	33.9 ± 6.1	26	3.143	2.181	1.070
10-2	10	2	59.4 ± 3.2	12	0.314	0.053	1.603
25-2	25	2	15.4 ± 5.3	10	0.786	0.484	1.090
50-2	50	2	23.3 ± 5.1	14	1.571	1.094	0.817
75-2	75	2	10.1 ± 1.7	14	2.357	1.815	0.719
100-2	100	2	36.3 ± 6.8	16	3.143	2.639	0.629
10-3	10	3	59.4 ± 3.2	11	0.314	0.062	1.303
25-3	25	3	16.9 ± 5.4	7	0.786	0.612	0.996
50-3	50	3	14.0 ± 4.7	8	1.571	1.318	0.884
75-3	75	3	9.9 ± 1.9	10	2.357	2.003	0.579
100-3	100	3	33.6 ± 6.7	13	3.143	2.644	0.350

Table 2. Equations used for mass and heat balance

Contents	Equation	
Airflow rate of outlet air (m³/h)	$V_{out} = \frac{(273.15 + T_{out})}{(273.15 + T_{in})} \times V_{in}$	(3)
Water vapor per unit air volume (g/m³)	$X = \frac{217 \times pv}{273.15 + T}$	(4)
Water vapor pressure (Pa)	$pv = RH \times pvs$	(5)
Saturated water vapor pressure (Pa)	$pvs = 6.1078 \times 10^{\frac{7.5 \times T}{T + 237.3}}$	(6)
Organic degradation	$C_{21}H_{36}O_{14}N + 22.3\ O_2 \rightarrow 21\ CO_2 + 16.3\ H_2O + NH_3 + Heat$	(7)
Generated CO_2 (kmol/h)	$\Delta C_{gen} = [(V \times CO_2)_{out} - (V \times CO_2)_{in}] \times \frac{1}{100} \times \frac{1\ kmol\ CO_2}{22.4\ m^3}$	(8)
Degraded organics (kg/h)	$\Delta M_O = \frac{1}{21} \times \Delta C_{gen} \times \frac{533.2\ kg}{1\ kmol}$	(9)
Metabolic water (kg/h)	$\Delta w_{gen} = \frac{16.3}{21} \times \Delta C_{gen} \times \frac{18\ kg}{1\ kmol}$	(10)
Heat generation (kJ/h)	$\Delta Q_{gen} = \Delta M_O \times 20406\ kJ/kg$	(11)
Heat transfer in air flow (kJ/h)	$\Delta Q = h_{dry} \times \rho_a \times V + h_{vapor} \times X \times 10^{-3} \times V$	(13)
Enthalpy of dry air (kJ/kg)	$h_{dry} = 1.006 \times T$	(14)
Enthalpy of water vapor (kJ/kg)	$h_{vapor} = 1.805 \times T + 2501$	(15)
Density of dry air (kg/m³)	$\rho_a = 1.293 \times \frac{273.15}{273.15 + T}$	(16)

Fig. 1 Schematic view of the reactor used in the bio-drying experiment

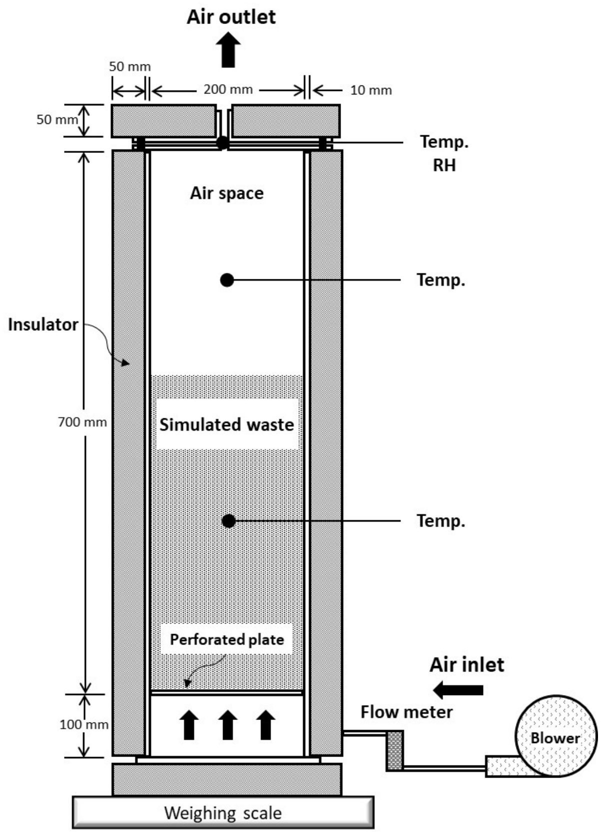

Fig.2 Experimental data and model output of run "50-3" (a) Temperature and CO_2 concentration profiles (Measured), (b) Rate of water mass changes in balance (Estimated), (c) Heat profiles (Estimated)

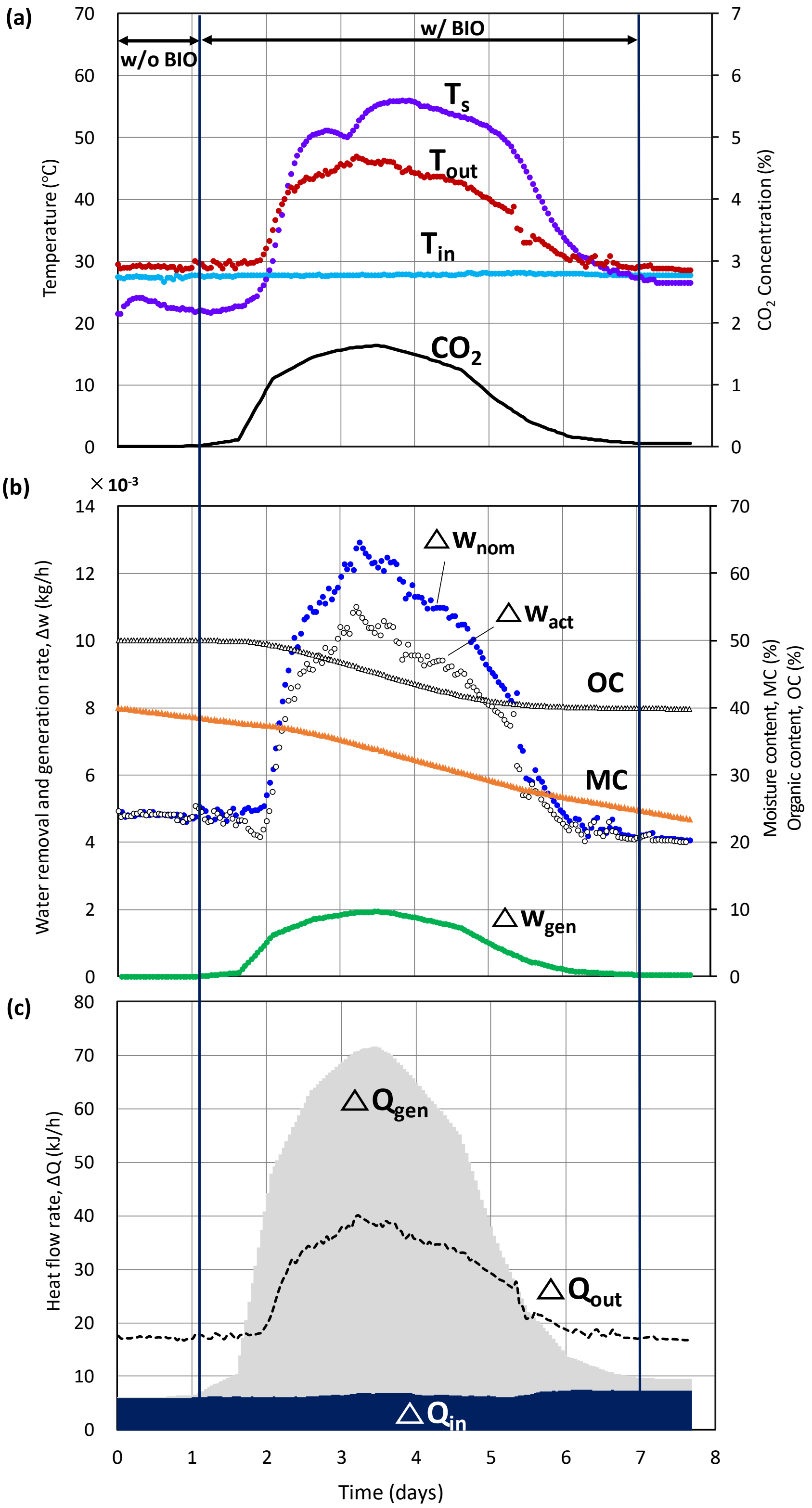

Fig. 3 Comparison of actual removed water mass (W_{act}) between experiment and model during entire experimental period

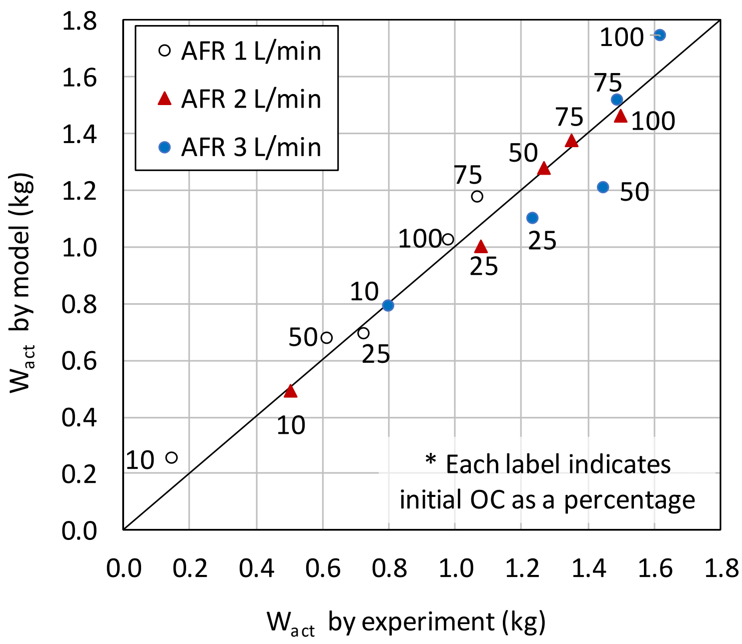

Fig. 4 Temperature dependence of pvs and X_{sat} and increase of water vapor pressure (pv) in bio-drying process

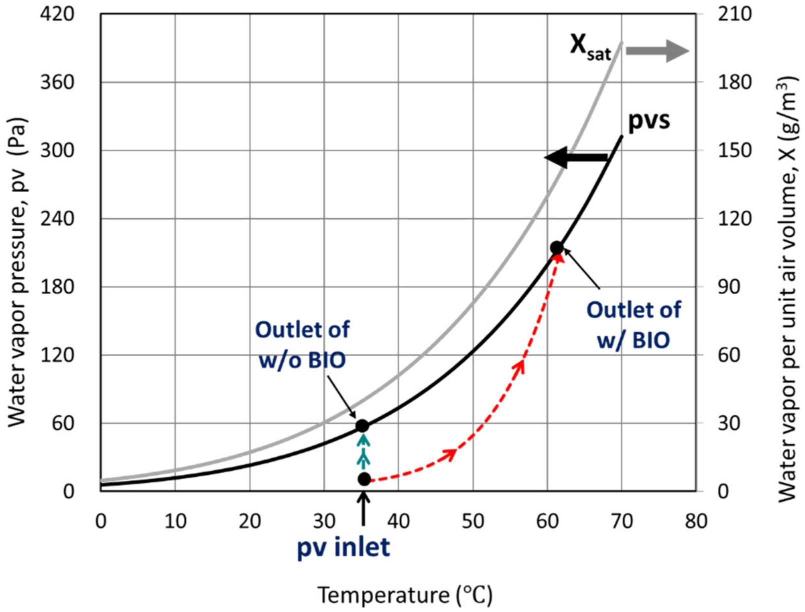

Fig. 5 Relations between water removal rate and RH of inlet air under different AFR during w/o BIO period

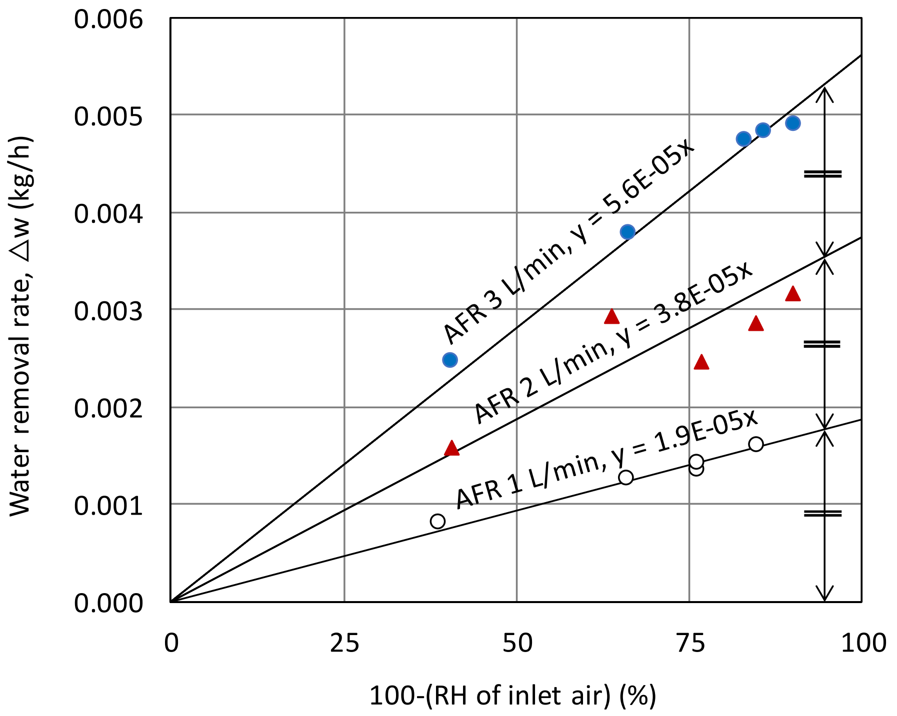

Fig. 6 CO_2 generation rate and moisture content profiles during entire experimental period (a) AFR 1 L/min, (b) AFR 3 L/min

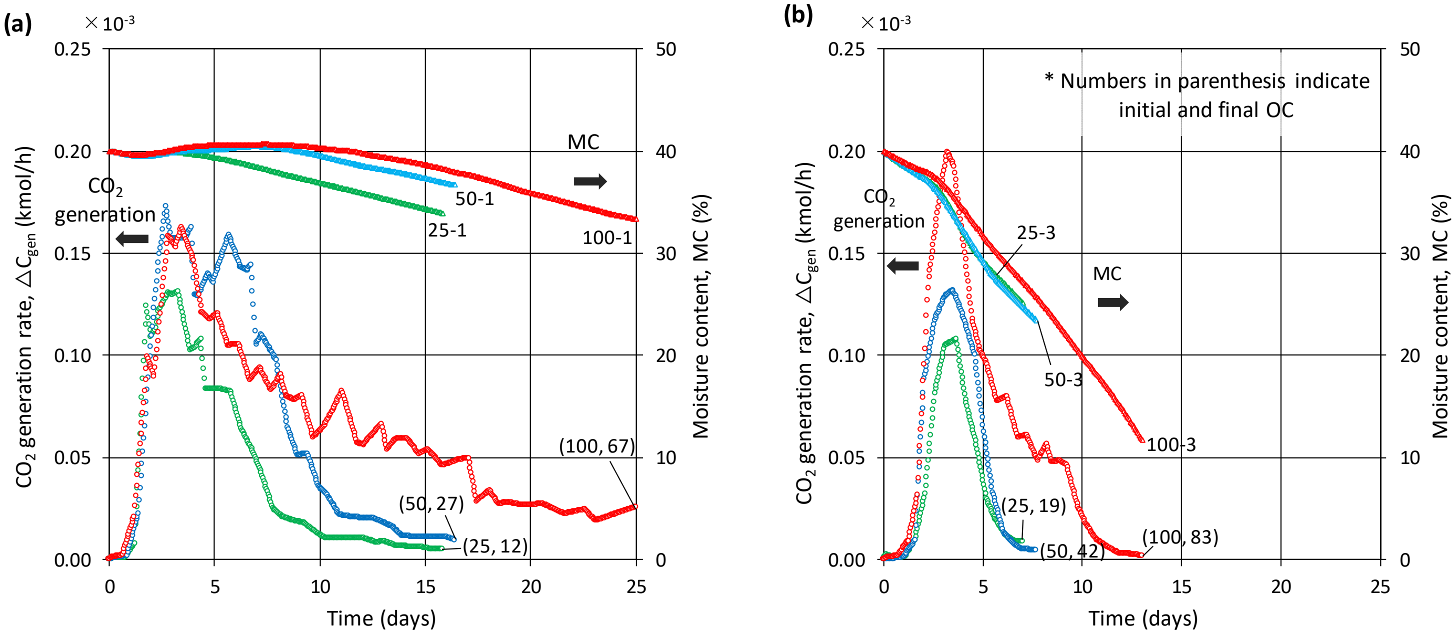

Fig. 7 Conceptual diagram of water removal rate in the bio-drying process

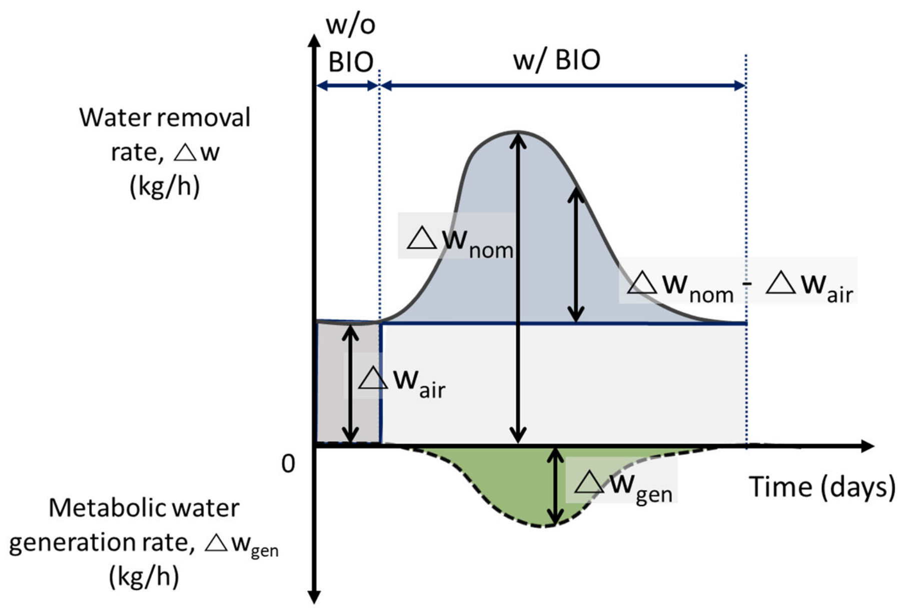

Fig. 8 Water removal rate defined in Fig. 7 at the peak point of CO_2 concentration (a) AFR 1 L/min, (b) AFR 3 L/min

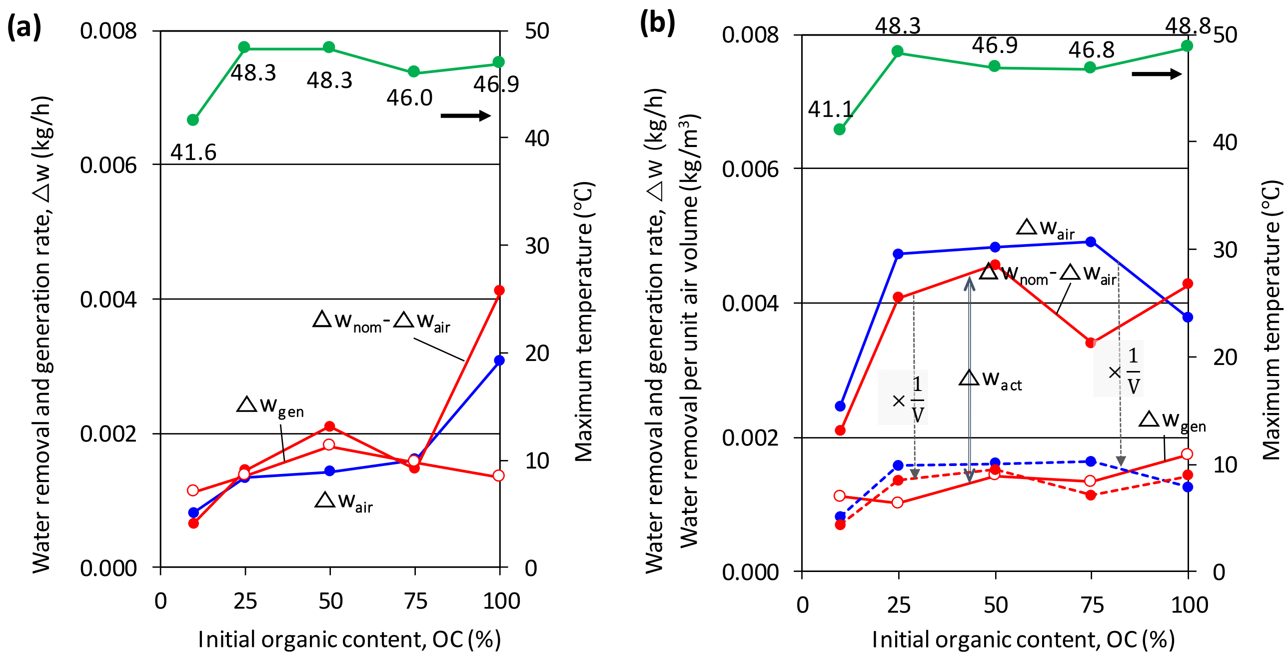

Fig. 9 Removed water mass during w/ BIO period (a) Comparison of nominal removed water mass (W_{nom}) and actual removed water mass (W_{act}), (b) Effect of temperature increase ($W_{nom}-W_{air}$, $W_{nom}-W_{air}-W_{gen}$) on water removal compared with the effect of airflow (W_{air})

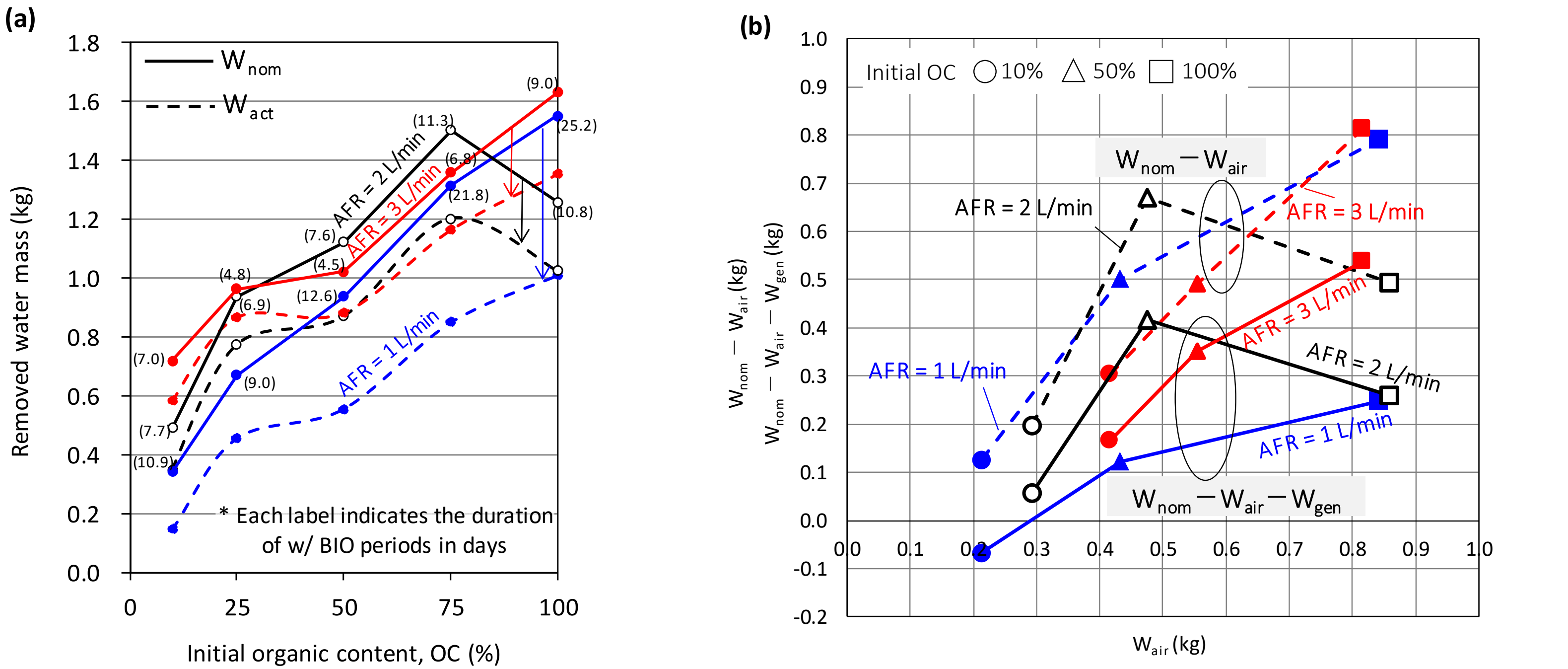

Fig. 10 Overall water removal mechanism in the bio-drying process